Antimicrobial Colloidal Suspensions of Silver-Titania

Stefania Gavriliu[*,1], Magdalena Lungu[1], Liana C. Gavriliu[2], Florentina Grigore[1] and Claudia Groza[1]

[1]*National Institute for Research and Development in Electrical Engineering ICPE-CA, Bucharest, Romania*

[2]*"Carol Davila" University of Medicine and Pharmacy, Bucharest, Romania*

Abstract: Titanium dioxide nanoparticles (TiO_2Np) exhibiting properties of photocatalyst under ultraviolet light (UV) exposition related with destruction of some hazardous organic moieties. To enhance the antibacterial characteristics of this material in our works, we developed a new method of TiO_2Np doping with silver nanoparticles (Ag^0Np), whose biocidal properties are well defined. The obtained products, Ag^0Np/TiO_2Np, in the form of suspensions and powders were characterized from chemical, physical and antimicrobial activity point of view. In addition, a mechanism of Ag^+ ions reduction reaction to Ag^0Np has been proposed. The developed method of the Ag^0Np/TiO_2Np synthesis consists of the *in situ* chemical deposition of the Ag^0Np on the dispersed TiO_2Np in the form of anatase, using aqueous solutions of poly(acrylic acid sodium salt) (PAS) and $NaBH_4$. The Ag^0Np synthesis was carried out both in the presence and absence of TiO_2Np. The chemical composition of Ag^0Np/TiO_2Np was assessed by atomic absorption spectrometrical method (AAS). The physical properties were evaluated as follows: crystallite structure and dimensions of nanopowders by X-ray diffraction method (XRD), UV-Vis absorption of colloidal suspensions and UV-Vis reflectance of nanopowders by spectrophotometrical method, grain size distribution of nanoparticles by dynamic light scattering method (DLS), stability of colloidal suspensions by zeta potential measurements, forms and shapes of Ag^0Np and Ag^0Np/TiO_2Np by transmission electronic microscopy (TEM) and scanning electronic microscopy (SEM) respectively. The antimicrobial activity was tested by standard methods against some broad spectra of fungi and bacteria. In suspensions, the concentration of TiO_2Np was 1 wt. % and the concentration of Ag^0Np varied in the range of 0.005…0.15 wt. %. The Ag^0Np suspensions and Ag^0Np/TiO_2Np suspensions were stable from the physical and chemical point of view. The physical characterization test results were in accordance, proving the achievement of colloidal solutions containing Ag^0Np and TiO_2Np spherical nanocrystallite with average diameters of 4.1 nm and 7.8 nm, respectively. The results of the biological tests showed the high fungistatic and antibacterial activities of both products in form of colloidal suspensions and powders. The developed "one pot method" is efficient, ecological and easy to be scaled-up. The obtained products have biological activity but it depends on the nature of the tested germs, lowering in the series: Gram negative bacteria, Gram positive bacteria and fungi. Also, a synergistic action was proved at destroying of *Trichoderma viride* fungus, which was not obtained either for Ag^0Np or for TiO_2Np, independently.

Keywords: Silver nanoparticles, titanium dioxide nanoparticles, antimicrobial activity.

1. INTRODUCTION

TiO_2Np and Ag^0Np are widely used materials due to their distinguished chemical and physical properties, which make them very attractive for applications such as catalysis, electronics, optics and biotechnology [1-6]. These properties are originated from intrinsic molecular and crystalline structures and their bulk and surface chemistry [7].

The tetragonal crystallites of anatase and rutile (the common forms of TiO_2), which are represented as octahedral structures of (TiO_2^{6-}), differ by the distortion of each octahedral and by assembly patterns of the octahedral chains, and in certain circumstances are available for changing by different entities absorption. Thus, TiO_2 is a n-type semiconductor due to oxygen vacancies, which are formed by the release of two electrons and molecular oxygen.

*Address correspondence to this author at the National Institute for Research and Development in Electrical Engineering ICPE-CA, Splaiul Unirii No. 313, Sector 3, 030138 Bucharest, Romania;
Tel: +40-021/3468297, Ext. 108; Fax: +40-021/3468299;
E-mails: stefgav@icpe-ca.ro, stefania_gavriliu@yahoo.com

The photoinduced phenomena (photocatalysis, photovoltaic and photosuperhidrophylicity) are activated by the input of super-band "gap energy". It is the energy difference between the valence and the conduction band produced by the absorption of a photon having enough energy to promote an electron from valence band to conduction band, which in turn, leads to charge separation of a hole (h^+) in the valence band and appearance of an electron-hole pair (e^- - h^+).

The photocatalysis is more likely to be sensitive to bulk properties while the photosuperhidrophylicity is an interfacial phenomenon. The catalysts have the ability to adsorb simultaneously two reactants, which are reduced and oxidized as follows:

$$\left(Ox_1\right)_{ads.} + \left(\mathrm{Re}\, d_2\right)_{ads.} \xrightarrow[h\nu > E_g]{\text{Semiconductor}} \left(\mathrm{Re}\, d_1\right) + \left(Ox_2\right) \qquad (1)$$

where E_g is band gap energy.

Anatase and rutile are used commonly as photocatalysts. Both have a lot of advantages in applications (chemically inert, photocatalytically stable, cheap, efficiently activated

1875-0389/09

by sunlight, easy to produce and use, and no hazardous for humans and environment) even in different grain size ranging from clusters, colloids and powders to large crystals. Anatase has a greater activity for most reactions. The photocatalyst activity is related with some hazardous organic moieties destroy and may be extended to antibacterial action, too. The biocidal action of TiO_2 against *E. coli*, *Lactobacillus acidophilus* and *Sacharomyces cerevisiae* was reported even since 1985 [8]. TiO_2 as a photocatalyst is more effective than any other antimicrobial agent because it does not only kill microbes, but also decomposes the cells themselves of bacteria, fungi, algae and viruses. The end toxins formed as a result of the cell death are decomposed by a photocatalytic action, too. Almost, any organic compound can be completely mineralized with irradiated TiO_2. This photodegradation is due to high oxidizing action of holes and hydroxyl radicals (HO*). The main pathway of microbial cell breakdown follows the reaction [7]:

$$\text{Microbial cell} \xrightarrow[h\nu > E_g]{TiO_2} CO_2 + H_2O + \text{Mineral acid} \quad (2)$$

The photocatalytic property of TiO_2 is properly manifested under UV light. Visible light really contains only 4 % of UV. For a high efficient photocatalysis are needed deep electron traps and high surface acidity to extend the life time of photoexcited electrons and holes, and to ensure better adsorption of organic substances on the surface. The well known ways to enhance the photocatalytic activity are to shift the absorption band gap edge to red in order to improve activity in the visible portion of spectra or to increase the photoactivity in the near and visible portion.

When TiO_2 is spiked with nitrogen ions, its photocatalytic action is enlarged under visible light [9]. The doping of TiO_2Np with different transition metals may lead to enhanced efficiency of the photocatalytic activity by increase the electron-rate to oxygen and thereby the quantum yield transfers [10].

Silver has been employed most extensively since ancient times to kill bacteria. Several papers tried to explain the inhibitory effects on Ag^+ ions/Ag^0 on bacteria, but the working mechanism was not fully investigated. It is generally accepted that Ag reacts with proteins by combining the thiol (-SH) groups, which leads to the inactivation of the bacterial cells [2-6].

Ag ions or elemental Ag were introduced into TiO_2 powders and films by different methods such as sol-gel method, mechanical mixing or chemical deposition, precipitation-reduction, photodeposition and as a result the photocatalytic activity was improved to varying extent [11-18].

There is expected that the deposition of Ag^0Np on TiO_2Np to be advantageously or detrimentally for photocatalytical activity, taking into account the dependence of this property upon a lot of factors involving quantity and quality of deposition, nature of the pollutant substance and working conditions. In these circumstances, there is an optimum loading value. For a higher Ag^0Np content, a decrease in electron density occurs, due to electron attraction by numerous metal nanoparticles. The resulting complicated field configuration has a detrimental effect on the charge separation, lowering the photocatalytical activity. In the same time, a higher content of Ag^0Np limits the amount of light which arrives on the surface of TiO_2Np, reducing the number of photogenerated hole-electron and lowering consequently the photodegradation of bacterial cell. The negatively Ag^0Np, especially for highly loaded TiO_2Np, attract holes and subsequently recombine them with electrons. In this manner the Ag^0Np become recombination centers.

In order to improve the antibacterial characteristics of TiO_2Np, in this paper we developed a new method of TiO_2Np doping with bioactive Ag^0Np. The obtained products were characterized from chemical, physical and antimicrobial activity point of view. Also, a mechanism of Ag^+ ions reduction reaction to Ag^0Np has been proposed.

2. MATERIALS AND METHODOLOGY

The experiments were carried out using the following starting materials:

- deionized water with conductivity of 18.2 MΩ·cm at 25°C obtained by a Simplicity UV water purification system Millipore, France;
- nanopowders of TiO_2, anatase, $TiO_2 \geq 99.5$ %, with the mean diameter of 7.8 nm, of Metall Rare Earth Limited, China;
- silver nitrate p.a., crystallized, $AgNO_3 \geq 99.9$ % of Fluka, Germany;
- poly(acrylic acid, sodium salt, PAS), $C_3H_3NaO_2$, with $M_w = 5{,}100$ of Aldrich, Germany;
- sodium borohydride, $NaBH_4 \geq 96$ % of Merck, Germany.

The method consists of an *in situ* chemical deposition of Ag^0Np from an $AgNO_3$ aqueous solution on TiO_2Np, which previously was dispersed in a PAS solution using an ultra sound bath. A stock aqueous solution of 0.1 M $AgNO_3$, which was diluted to concentrations of 1 - 10 mM as source of Ag^+ ions was used. The deposition was realized in an ultra pure N_2 stream to remove the O_2 traces, using in the first step a soft reduction of Ag^+ ions with PAS by refluxing the TiO_2Np suspension containing Ag^+ ions. The refluxing was maintained to a milky yellow color appeared. In the second step, the suspension was cooled at 4°C and the reduction reaction was finalized by adding of a $NaBH_4$ cold solution in an $AgNO_3$: $NaBH_4$ molar ratio of 1:2.

In order to obtain Ag^0Np/TiO_2Np in form of concentrated slimes or powders, the obtained suspension may be centrifuged to the desired wet content and a drying may be carried out, respectively.

The final products were characterized from the followings points of view: chemical composition using a SOLAAR S4 - Thermo Electron Corporation (UK) apparatus, crystalline structure and crystallite dimensions by X-ray diffraction using a D8 Advance - Bruker AXS (Germany) diffractometer, UV-Vis reflectance and absorbance using a spectrophotometer of V-570 Jasco (Japan) type having an integrative sphere, grain size distribution and stability using a 90 PLUS Brookhaven (USA) apparatus, shape and dimensions of nanoparticles

using a transmission electronic microscope of Philips CM100 (Holland) type and a scanning electronic microscope of Philips XL 30 (Holland) type.

The antifungal effectiveness was tested by antibiogram method, according to the conditions of IS 60068-2-10, sixth edition 2005-06 standard, upon Ag^0Np/TiO_2Np samples in form of powder, using a mould mixture of *Aspergillus species* (niger, fumigatus, flavus, versicolor and terreus), *Paecilomyces varioti*, *Aureobasidium pullulans*, *Penicillium* species (glaucum and citricum), *Stachybotrys atra*, *Trichoderma viride* and *Scopulariopsis brevicaulis* germs.

The antibacterial activity tests were carried out upon Ag^0Np, TiO_2Np and Ag^0Np/TiO_2Np samples in form of colloidal suspension or powder by microdilution method, according to the standards in force, against some common and aggressive bacterial strains (*Staphylococcus aureus* ATCC 25923, *Escherichia coli* ATCC 25922, *Enterobacter cloacae* ATCC 13047, *Acinetobacter baumannii* ATCC 17978, *Candida albicans* ATCC 10231, *Pseudomonas aeruginosa* ATCC 27853, noticed as I, II, III, IV, V, and VI, respectively.

3. RESULTS AND DISCUSSION

The use of different kinds of counter ions of polyelectrolytes in the polymeric protected synthesis of metal nanoparticles is a way for obtaining of highly concentrated colloidal suspensions [19]. Polymethylmet-acrylic ammonium salt, polyacrylic ammonium salt and polyacrylic sodium salt were reported as suitable stabilizers for obtaining of Ag^0Np colloidal suspensions using Ag^+ ions reduction methods by chemicals such as N_2H_4, $NaBH_4$, photoreduction, thermal decomposition or gamma radiation [20-23].

The polar nature of TiO_2 nanocrystallite surface facilitates the strong adsorption of ions or charged molecules through electrostatic interaction. An efficient dispersion of TiO_2Np is obtained by an electrostatic preferential adsorp-tion of PAS, which is a polysalt of negatively charged polyelectrolyte of "weak" type.

The possible processes and chemical reactions may be described as follows in Scheme **1**.

The carboxylate ligands bond strongly the Ag^+ ions which are likely to become trapped in the bulk of material and on the surface of the particles. The above repeating units, $-CH_2-CH(COOAg^+)-$ are some real nanoreactors for Ag^+. In a first stage of synthesis, the Ag^+ ions are reduced in form of Ag^0 germs or nanoclusters by heating. The reduction is a photocatalytic reaction, which uses the fresh formed metal crystallites rich in photoproduced electrons as sites for cathodic-like reduction of Ag^+ ions. In this manner the crystallites grow progressively as presented in Eq. (3):

$$Ag^0 + Ag^+ \rightarrow (Ag_2)^+ \xrightarrow{e^-} Ag_2 \xrightarrow{Ag^+} (Ag_3)^+ \rightarrow ...Ag_n \qquad (3)$$

The preferential adsorption of Ag^+ positive ions by negative ions of PAS on the TiO_2Np and the capped Ag^+ ions are presented in Fig. (**1**).

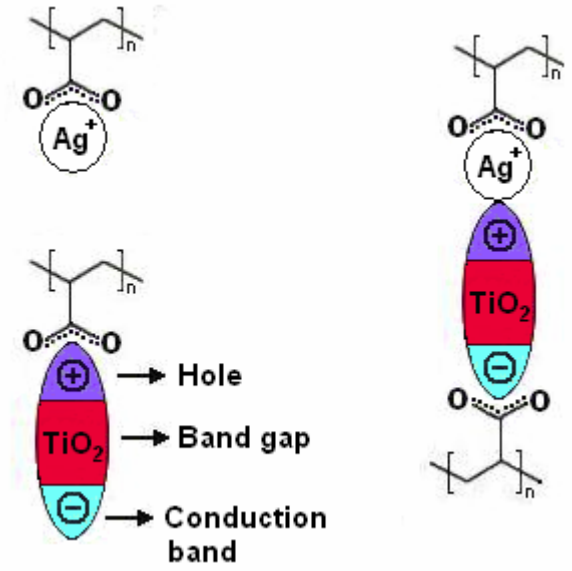

Fig. (1). Electrostatic bonding of TiO_2Np and Ag^+ ion by negative ions of PAS.

The use of only a soft reduction lengthens reaction time. Thereof, a second stage of reduction was performed using a strong reductive agent such as $NaBH_4$. The reaction occurs following the equation (4):

$$2Ag^+ + BH_4^- + 3H_2O \rightarrow 2Ag^0 + H_2BO_3^- + 2H^+ + 3H_2 \qquad (4)$$

In such a case, the above nanoparticle grow by autocatalytic reduction of Ag^+ on the Ag^0Np surface freshly prepared is limited and after the reduction some uniform sized Ag^0Np are formed. In the same time, higher Ag^0Np concentrations could be obtained comparatively with others

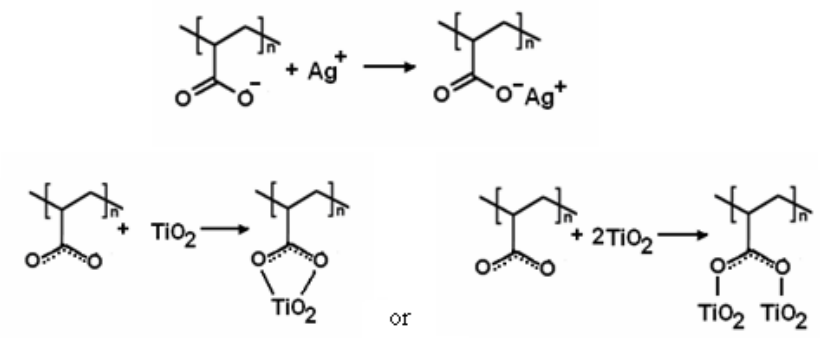

Scheme 1.

reduction conditions. The presence of anchoring groups of carboxylate type from PAS plays the major role in the deposition of Ag^0Np on TiO_2Np surface, as well as in the electron transfer process. Also, the anchoring groups broaden the absorption of photons in the visible region of spectra and improve the electron injection efficiency of Ag^0Np into the conduction band of TiO_2Np. The red shift is attributable mainly to electron transfer from the surface plasmon of Ag^0Np to the conduction band of colloidal TiO_2.

The doping of TiO_2Np with Ag^0Np, practiced in our work, is advantageously for surface sensitization of the wide-band gap of TiO_2Np by electrons transfer because of increasing the efficiency of excitation processes and expanding the used wavelength range. The electron-hole separation is improved as a result of electron donation or acceptance, depending on the redox environment.

As the work function of Ag is higher than TiO_2 (Ag: 4.52-4.74 eV against Ti: 4.33 eV), electrons are removed from the TiO_2Np to vicinity of each Ag^0Np, leading to a Schottky barrier at each metal semiconductor region, which in turn leads to a decrease in electron-hole recombination and an efficient charge separation.

Possible aspects of Ag^0Np/TiO_2Np electrostatic protection by negative ions of PAS are presented in Fig. (**2**).

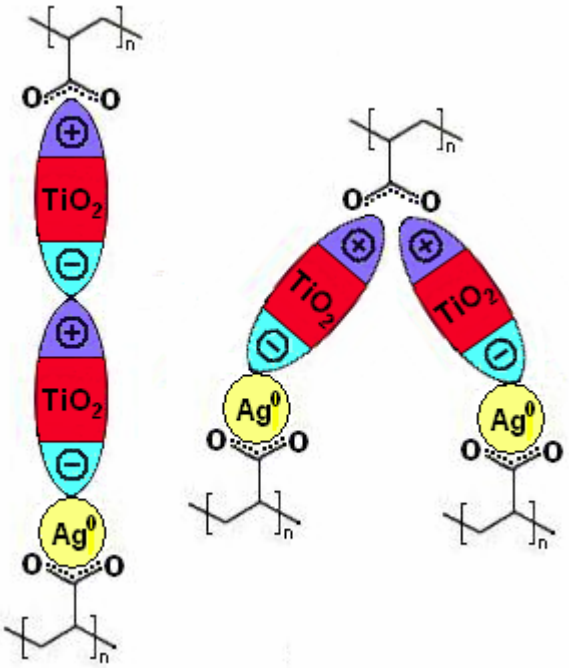

Fig. (2). Ag^0Np/TiO_2Np electrostatic protection by negative ions of PAS.

In our works, we prepared some Ag^0Np/TiO_2Np composite powders samples in the form of suspensions containing 1 wt. % TiO_2Np and 0.005 wt. %, 0.01 wt. %, 0.1 wt. % or 0.15 wt. % Ag^0Np, respectively.

Further, we refer only to the Ag^0Np/TiO_2Np sample containing 1 wt. % TiO_2Np and 0.005 wt. % Ag^0Np, respectively, because the others have approximately the same characteristics. The physical characteristics and the antifungal activity of this sample are presented in Figs. (**3**, **11**, **12**, **13**), respectively. Table **1** presents comparatively the antibacterial activity of suspensions of TiO_2Np, Ag^0Np and Ag^0Np/TiO_2Np.

These solutions were stable and this fact can be observed in Figs. (**3**, **4**) by zeta potential values of – 49.83 mV for the Ag^0Np solution and of – 35.21 mV for the Ag^0Np/TiO_2Np suspension.

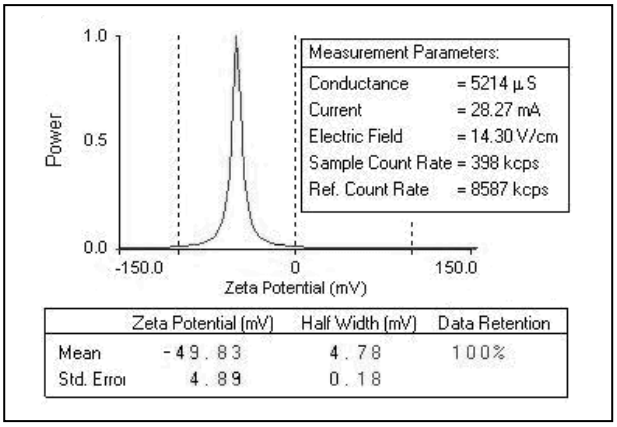

Fig. (3). Zeta potential of the Ag^0Np solution.

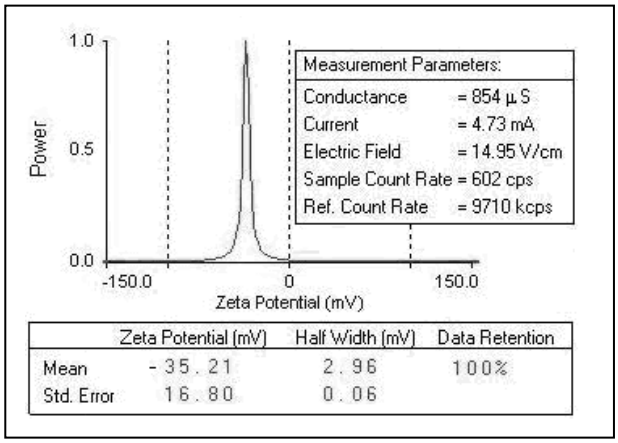

Fig. (4). Zeta potential of the Ag^0Np/TiO_2Np suspension.

Fig. (**5**) presents the XRD pattern of Ag^0Np/TiO_2Np powder obtained from the suspension containing 1 wt. % TiO_2Np and 0.005 wt. % Ag^0Np.

X-ray structure analysis of Ag^0Np/TiO_2Np powder showed that it has typical peaks of TiO_2Np polycrystalline anatase well crystallized, without any detectable Ag^0Np peaks. This is due to the very small content of the Ag^0Np (0.0009 at. %), which is situated below the detection limit for XRD (1 at. %). The tetragonal Bravais lattice type was also verified by lattice constant calculated from these peaks. Based on the full width at half maxima of the XRD peaks, the average particle diameter was calculated to be about 7.8 nm by using Scherrer's formula. There was no measurable effect on the size of TiO_2Np with the addition of Ag^0Np in the studied range.

Fig. (**6**) presents comparatively UV-Vis absorbance spectra of the suspensions containing 0.005 wt. % Ag^0Np, 1 wt. % TiO_2Np and Ag^0Np/TiO_2Np with 0.005 wt. % Ag^0Np and 1 wt. % TiO_2Np.

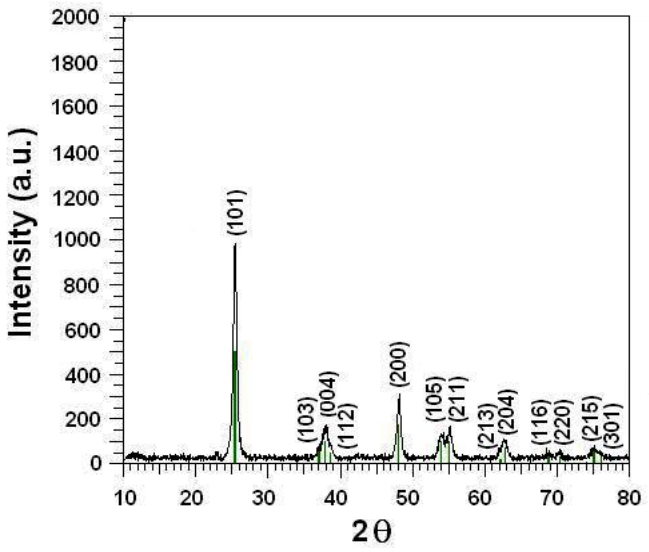

Fig. (5). XRD pattern of Ag^0Np/TiO_2Np powder.

UV-Vis spectroscopy is one of the most widely used techniques for characterization of Ag^0Np from structural point of view. The interesting optical properties of Ag^0Np are mainly based on their surface plasmon resonance (SPR), which appear under a light having a wavelength closed to Ag^0Np dimensions. In these circumstances it can cause the oscillation of conduction electrons in crystalline nanoparticles. Surface plasmon bands appearing in the visible region are characteristics of the Ag^0Np. Mie's theory predicts only a single SPR band in the absorption spectrum of spherical metal nanoparticles. The position and shape of the plasmon absorption of nanoparticles are strongly dependent on the particle size, dielectric medium and surface adsorbed species [24].

The absorption spectrum from Fig. (**6**) of the suspension with 0.005 wt. % Ag^0Np (curve 1) shows a maximal absorption at 408 nm indicating the presence of spherical Ag^0Np with a narrow size range. The minimal absorption from 326 nm corresponds to the wavelength at which the real and imaginary parts of the dielectric function of silver almost vanish [18]. Both the grain size distribution measured by DLS (Fig. **7**) and the TEM imaging (Fig. **8**) confirm this. The predominant family of Ag^0Np has particle sizes between 3.57 nm and 8.85 nm and their mean diameter is of 4.1 nm. Also, there is a tail towards the larger particle size between 31.59 nm and 194.47 nm in a very low amount, which is negligibly and can be removed partially by centrifugation and filtration.

The Ag^0Np absorption (Fig. **2**, curve 1) is red shifted by doping of TiO_2Np from 408 nm to 452 nm (Fig. **6**, curve 3). Also, the absorption spectra from Fig. (**6**, curve 2 and curve 3) present a very low red shift of two maximal absorptions of Ag^0Np/TiO_2Np against TiO_2Np (from 344 nm to 345 nm and from 373 nm to 376 nm). The SRP of TiO_2Np from 423 nm and 686 nm are strong and very strong, respectively amplified by Ag^0Np deposition.

The effect of Ag^0Np loading on the band energy of TiO_2Np was investigated using diffuse reflectance spectroscopy method in UV-Vis. The comparison of the spectra of TiO_2Np and Ag^0Np/TiO_2Np powders from Fig. (**9**) indicates that the deposition of Ag^0Np on TiO_2Np even in very low Ag^0Np amounts (of 0.1 wt. %) decreases the reflectance with about 8 % at 400 nm. In the visible region of the spectra the Ag^0Np loading does not change noticeable the band energy of TiO_2Np. In these circumstances, it is not expected an improvement of TiO_2Np bacterial activity by change of band energy, but only by alone antibacterial activity of the Ag^0Np/TiO_2Np.

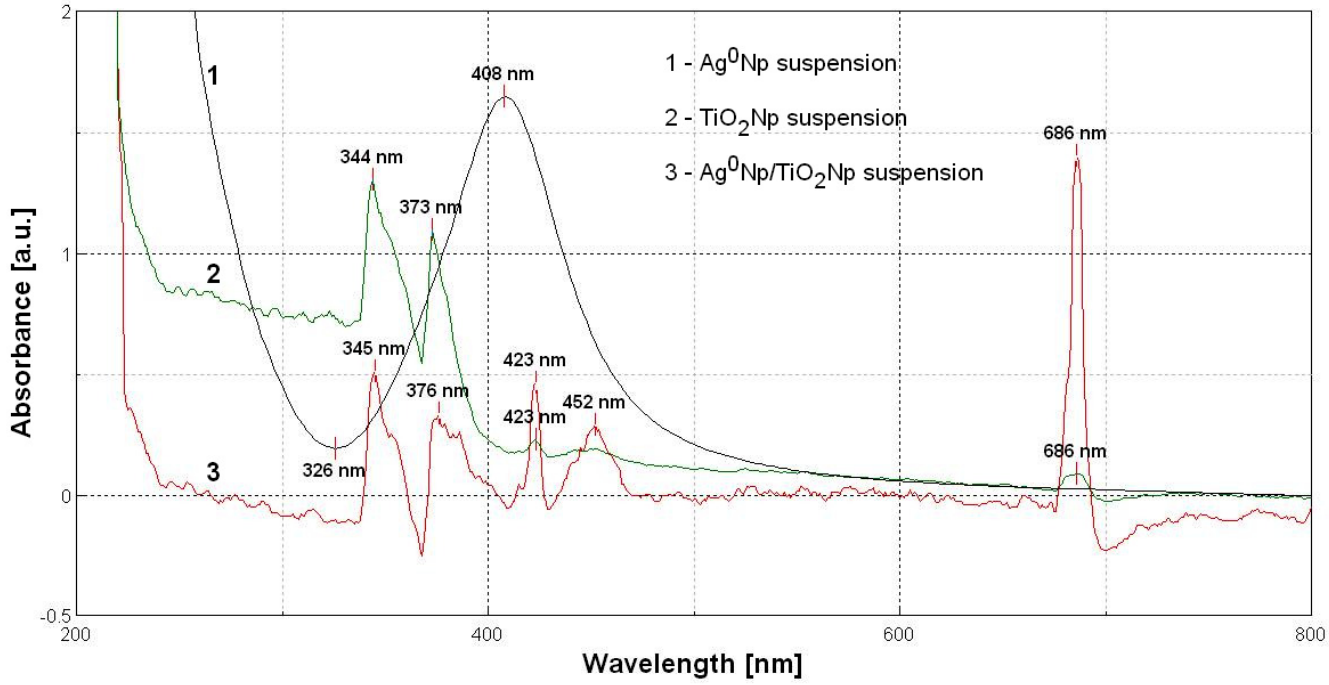

Fig. (6). UV-Vis absorbance spectra of the suspensions containing 0.005 wt. % Ag^0Np (1), 1 wt. % TiO_2Np (2) and Ag^0Np/TiO_2Np with 0.005 wt. % Ag^0Np and 1 wt. % TiO_2Np (3).

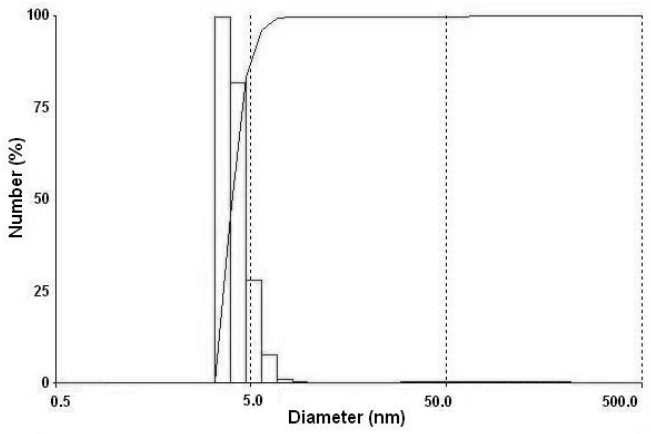

Fig. (7). Grain size distribution of the Ag^0Np from solution.

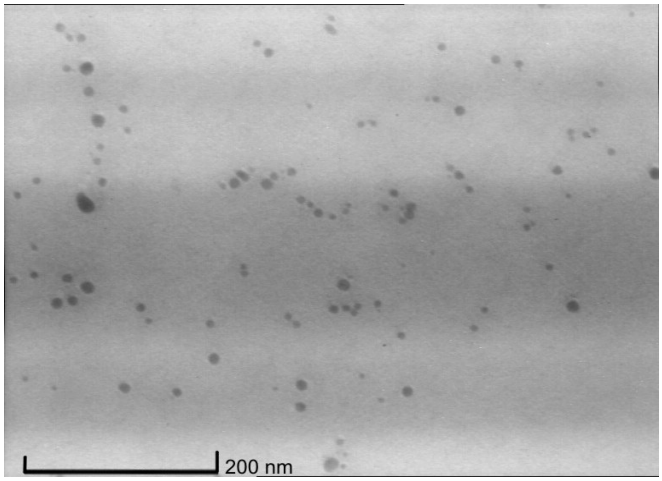

Fig. (8). TEM image of the Ag^0Np from Ag^0Np solution.

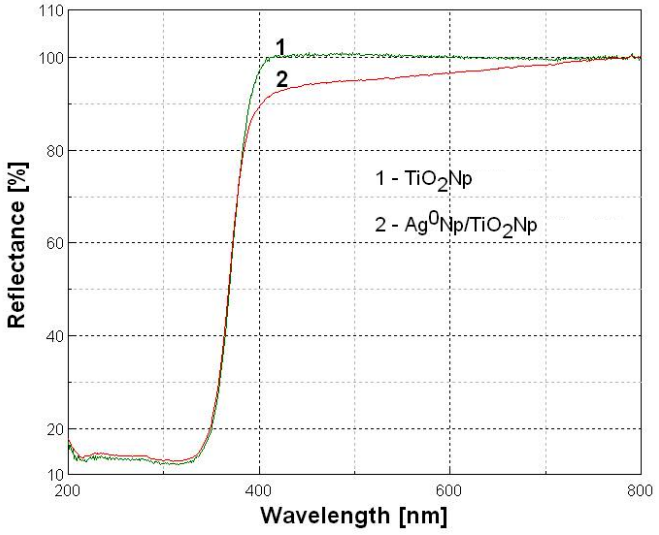

Fig. (9). UV-Vis reflectance spectra of TiO_2Np and Ag^0Np/TiO_2Np.

Fig. (**10**) presents the grain size distribution of the Ag^0Np/TiO_2Np from suspension. The DLS results from Fig. (**10**) show that in the predominant family the nanoparticles are distributed in the range of 8.11 nm and 11.63 nm having a mean diameter of 9.2 nm. There is a short tail towards the larger particle size situated between 49.31 nm and 77.49 nm.

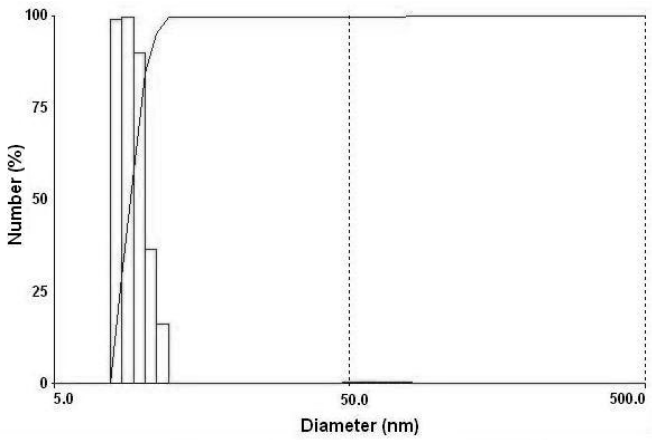

Fig. (10). Grain size distribution of the Ag^0Np/TiO_2Np from suspension.

The surface morphology of the Ag^0Np/TiO_2Np composite powder was examined by SEM (Fig. **11**). The micrograph confirms the nanometer size of the particles in the form of spheres. As SEM micrographs give only a rough measure of the particle size and the Ag^0Np amount is very low, they cannot be observed and as a result the images of the TiO_2Np loaded and un-loaded with Ag^0Np are similar.

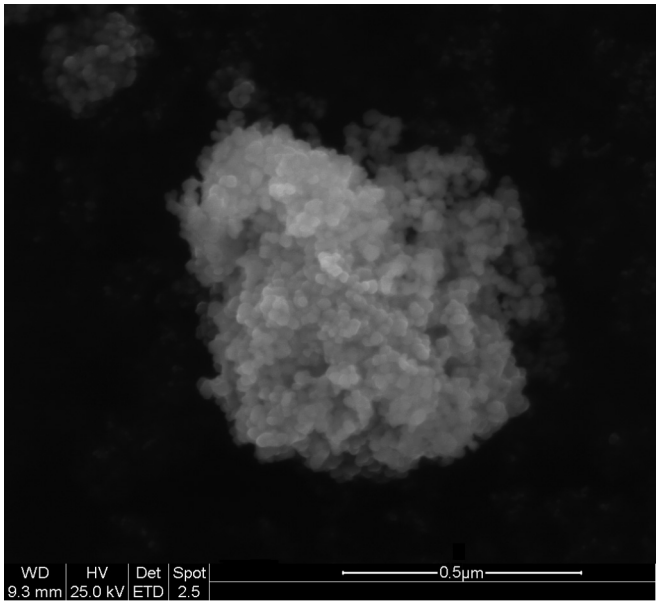

Fig. (11). SEM image of the Ag^0Np/TiO_2Np composite powder.

The data supplied by DLS and SEM measurements proved that the Ag^0Np deposition on the TiO_2Np does not change noticeably the dimensions, shapes and the grain size distribution of the nanoparticles support. The physical characterization test results are in a whole accordance, proving the achievment of an intimate Ag^0Np deposition on TiO_2Np.

Figs. (**12-14**) present comparatively the antifungal activity of TiO_2Np powder, Ag^0Np suspension having the concentration of 0.005 wt. % and Ag^0Np/TiO_2Np composite powder with 0.1 wt. % Ag^0Np.

Fig. (**12a**) shows that after three days the TiO_2Np powder has only a fungistatic action against all the tested moulds. *Trichoderma viride* begins to grow on the powder after

seven days, and at fourteen days (Fig. **12b**) it has the tendency to cover continuously the powder. Also, the fungistatic action against the other moulds is kept. There is not a visible consumption of TiO_2Np powder but a covering with moulds begins from borders of the sample.

(**a**)

(**b**)

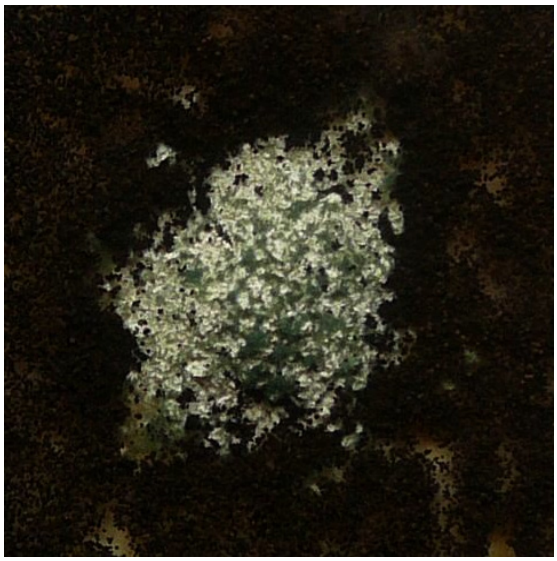

Fig. (12). The aspect of TiO_2Np powder after three days (**a**) and fourteen days (**b**) from inoculation with a mixture of the tested moulds.

Fig. (**13a**) shows that after three days the Ag^0Np suspension has a fungistatic action against all the tested moulds. *Aspergillus niger* and *Paecilomyces varioti* begin to grow with a high rate around the sample after seven days. After fourteen days (Fig. **13b**) we can observe that appearance of a visible consumption of the Ag^0Np can be observed, but the fungistatic action is kept against the all tested moulds excepting *Thrichoderma viride*.

Fig. (**14a**, left panel) shows that after three days the Ag^0Np/TiO_2Np composite powder has a fungistatic action against all the tested moulds. The surrounding of the sample has an opaque zone of 2…4 mm. After seven days, on the opaque zone Trichoderma viride begins to grow, and after fourteen days (Fig. **14b**, right panel), it covers continuously this zone. Also, it can be observed that a visible consumption of the Ag^0Np appears by their release in liquid medium, followed by chemical interaction with fungal germs. The fungistatic action is kept against the all tested moulds.

(**a**)

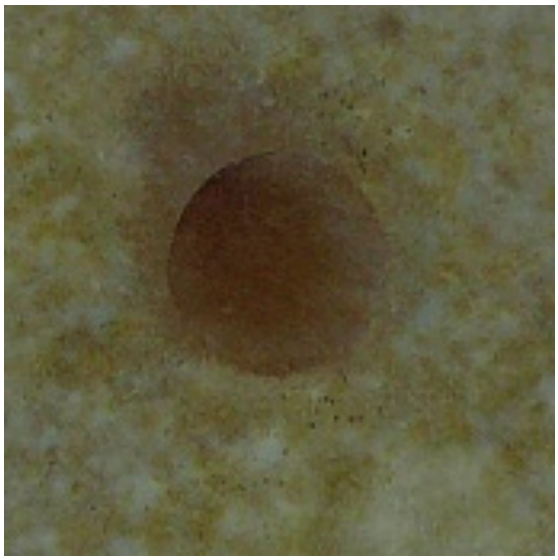

(**b**)

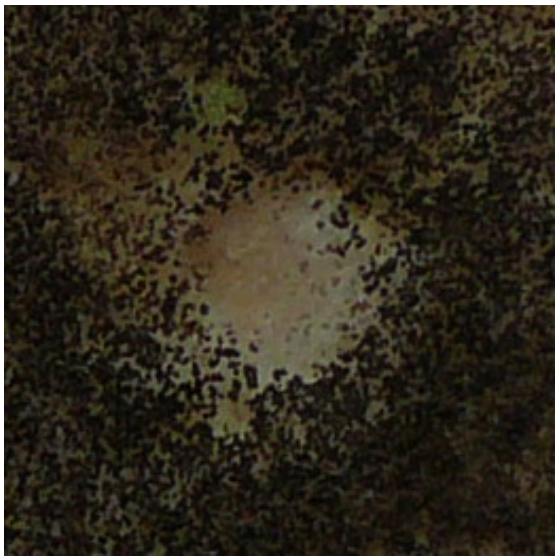

Fig. (13). The aspect of Ag^0Np suspension after three days (**a**) and fourteen days (**b**) from inoculation with a mixture of the tested moulds.

These results show that the antibacterial activity of TiO_2Np is based on a photocatalytic reaction while the antibacterial activity of Ag^0Np is based on the chemical reactions with microbial cells. Also, a synergistic effect against *Trichoderma viride* fungus was proved for Ag^0Np/TiO_2Np composite powders, which is not obtainable either for Ag^0Np or for TiO_2Np independently.

Table **1** presents comparatively the antibacterial activity of some suspensions containing Ag^0Np, TiO_2Np or Ag^0Np/TiO_2Np.

Table 1. Minimum Inhibitory Concentration (MIC) of Some Suspensions Containing Ag^0Np, TiO_2Np or Ag^0Np/TiO_2Np

Sample	Chemical Composition, wt. %		MIC of Ag^0Np, ppm					
	TiO_2	Ag^0Np	I	II	III	IV	V	VI
TiO_2Np colloidal suspension	1	0	R*	R	R	R	R	R
Ag^0Np colloidal suspension	0	0.005	24.68	20.82	20.82	24.68	20.82	20.82
Ag^0Np/TiO_2Np suspension	1	0.005	20.82	15.88	15.88	20.82	15.88	15.88

R* = resistant.

All the tested germs are resistant in the 1 wt. % TiO_2Np suspension, but in a suspension containing 10 wt. % TiO_2Np the MIC is of 300,000 ppm (3 wt. %).

(**a**)

(**b**)

Fig. (14). The aspect of Ag^0Np/TiO_2Np composite powder after three days (**a**) and fourteen days (**b**) from inoculation with a mixture of the tested moulds.

The MIC is greater for the Gram-positive germs (*Staphylococcus aureus* ATCC 25923 and *Acinetobacter baumannii* ATCC 17978) against the Gram-negative ones (*Escherichia coli* ATCC 25922, *Enterobacter cloacae* ATCC 13047 and *Pseudomonas aeruginosa* ATCC 27853). These are due to the differences between the compositions of the bacterial cell wall, which for Gram-positive bacteria consists of a thick multi-layer of peptidoglycan (a mixture of sugars and amino acids) and for Gram-negative bacteria consists of a thin and surrounded by an outer membrane (made up of lipopolysaccharides and lipoprotein).

The obtained colloidal suspension proved high antibacterial action and a fungistatic effect.

The new obtained products are more effective than Ag^0Np and TiO_2Np as a result of the cumulative effects in any illumination conditions.

4. CONCLUSIONS

The developed "one pot method" is highly efficient, ecological friendly and easy to be scaled-up. The obtained products have biological activity but it depend on the nature of the tested germs, lowering in the following series: Gram negative bacteria > Gram positive bacteria > fungi. Also, a synergistic action was proved at destroying of *Trichoderma viride* fungus, which was not obtained either for Ag^0Np or for TiO_2Np, independently.

ABBREVIATIONS

Ag^0Np	=	Silver nanoparticles
Ag^0Np/TiO_2Np	=	Silver nanoparticles deposited on titanium dioxide nanoparticles
DLS	=	Dynamic light scattering
MIC	=	Minimum inhibitory concentration
PAS	=	Poly(acrylic acid sodium salt)
SEM	=	Scanning electronic microscopy
SPR	=	Surface plasmon resonance
TEM	=	Transmission electronic microscopy
TiO_2Np	=	Titanium dioxide nanoparticles
UV	=	Ultraviolet light

REFERENCES

[1] Rengaraj, S.; Yeon, J.W.; Li, X.Z.; Jung, Y. Heterogeneous photocatalytic degradation of chlorophenols over Ag-TiO_2 nano particles in an aqueous suspension. *Solid State Phenomen.,* **2007**, *124 - 126*, 1745.

[2] Liu, H.R.; Ye, R.F.; Song, L.; Chen, Q. Structure and antibacterial properties of Ag-doped TiO_2 porous materials. *Key Eng. Mat.*, **2007**, *330 - 332*, 995.

[3] Holladay, R.J.; Christensen, H.; Moeller, W. Treatment of humans with colloidal silver composition, U.S. Patent 7,135,195, November 14, 2006.

[4] Siddhartha, S.; Tanmay, B.; Arnab, R.; Gajendra, S.; Ramachandrarao, P.; Debabrtata, D. Characterization of enhanced antibacterial effects of novel silver nanoparticles. *Nanotechnology*, **2007**, *18*, 225103.

[5] Kyung-Hwan, C.; Jong-Eun, P.; Tetsuya, O.; Soo-Gil, P. The study of antimicrobial activity and preservative effects of nanosilver ingredient. *Electrochim. Acta*, **2005**, *51*, 956.

[6] Pal, S.; Tak, Y.K.; Song, J.M. Does the antibacterial activity of silver nanoparticles depend on the shape of the nanoparticle? a study of the gram-negative bacterium *Escherichia coli*. *Appl. Environ. Microbiol.*, **2007**, *73*, 1712.

[7] Carp, O.; Huisman, C.L.; Reller, A. Photoinduced reactivity of titanium dioxide. *Progr. Solid State Chem.*, **2004**, *32*, 33.

[8] Matsungata, T.; Tomato, R.; Nakajima, T.; Wake, H. Photoelectrochemical sterilization of microbial cells by semiconductor powders. *FEMS Microbiol. Lett.,* **1985**, *29, 211*.

[9] Di Valentin, C.; Finazzi, E.; Pacchioni, G, Selloni, A.; Livraghi, S.; Paganini, A. C.; Giamello, E. N-doped TiO_2: theory and experiment. *Chem. Phys.*, **2007**, *339*, 44.

[10] Gerischer, H.; Heller, A. Photocatalytic oxidation of organic molecules at TiO_2 particles by sunlight in aerated water. *J. Electrochem. Soc.*, **1992**, *139,* 113.

[11] Coleman, H.M.; Marquis, C.P.; Scott, J.A.; Chin, S.– S.; Amal, R. Bactericidal effects of titanium dioxide-based photocatalysts. *Chem. Eng. J.*, **2005**, *113,* 55.

[12] Chang, G.; Zheng, X.; Chen, R.; Chen, X.; Chen, Z. Silver nanoparticles filling in TiO_2 hollow nanofibers by coaxial electrospinning. *Acta Phys. Chim. Sinica*, **2008**, *24*, 1790.

[13] Anandan, S.; Kumar, P. S.; Pugazhenthiran, N.; Madhavan, J.; Maruthamuthu, P. Effect of loaded silver nanoparticles on TiO_2 for photocatalytic degradation of acid red 88. *Solar Energy Mater. Solar Cells* , **2008**, *92*, 929.

[14] Kumar, V.K.; Porkodi, K. Comments on "Photocatalytic properties of TiO_2 modified with platinum and silver nanoparticles in the degradation of oxalic acid in aqueous solution". Langmuir Hinshelwood kinetics—A theoretical study. *Appl. Catal. B*, **2008**, *79*, 108.

[15] He, X.; Zhao, X.; Liu, B. Studies on a possible growth mechanism of silver nanoparticles loaded on TiO_2 thin films by photoinduced deposition method. *J. Non-Cryst. Solids*, **2008**, *354*, 1267.

[16] Liu, J.; Li, X.; Zuo, S.; Yu, Y. Preparation and photocatalytic activity of silver and TiO_2 nanoparticles/montmorillonite composites. *Appl. Clay Sci.*, **2007**, *37*, 275.

[17] Iliev, V.; Tomova, D.; Bilyarska, L.; Eliyas, A.; Petrov, L. Photocatalytic properties of TiO_2 modified with platinum and silver nanoparticles in the degradation of oxalic acid in aqueous solution. *Appl. Catal. B,* **2006***, 63,* 266.

[18] Keleher, J.; Bashant, J.; Heldt, N.; Johnson, L.; Li, Y. Photo-catalytic preparation of silver-coated TiO_2 particles for antibacterial applications, *J. Microbiol. Biotechnol.,* **2002**, *18*, 133.

[19] Chou, K.-S.; Chang, S.-C.; Huang, K.-C. Study on the characteristics of nanosized nickel particles using sodium borohydride to promote conversion. *Azo. J. Mat. Online,* **2007**, *3*, 1.

[20] Ryu, B.H.; Lee, J.D.; Lee, O.S.; Kang, Y.C.; Park H.S. Synthesis of highly concentrated silver nanoparticles assisted polymeric dispersant. *Key Eng. Mat.,* **2004**, *264*, 141.

[21] Hussain, I.; Brust, M.; Papworth, A.J.; Cooper, A. I. Preparation of acrylate-stabilized gold and silver hydrosols and gold−polymer composite films. *Langmuir*, **2003**, *19*, 4831.

[22] Narendra, S.; Khanna, P.K. In situ synthesis of silver nano-particles in polymethylmethacrylate. *Mat. Chem. Phys.,* **2007**, *104,* 367.

[23] Guillet, J.E. Cross-linked polymeric nanoparticles and metal nanoparticles derived therefrom, U.S. Patent, 7,189,279, March 13, 2007.

[24] He, R.; Qian, X.; Yin, J.; Zhu, Z. Preparation of polychrome silver nanoparticles in different solvents. *J. Mater. Chem.*, **2002**, *12*, 3783.

Received: February 22, 2009 Revised: March 19, 2009 Accepted: March 30, 2009